Elaboration and experimental validation of a Monte Carlo source model for linac 6 MV photon beams with and without Flattening Filter

Zakaria Aboulbanine[a,b,*], Karim Bahhous[a,c]

[a]*Faculty of Science, University Mohammed V in Rabat, Rabat, Morocco*
[b]*Deutsches Elektronen-Synchrotron DESY, Zeuthen, Germany*
[c]*Hassan II Oncology Centre, University Hospital Mohammed VI, Oujda, Morocco*

ARTICLE INFO

ABSTRACT

The concept of virtual source model has been developed to provide an efficient and precise particle generator mainly involved in standard photon beam treatment planing and Monte Carlo dosimetry simulations. In this work, we propose a source model for 6 MV linac photon beam for both irradiation modes, with and without flattening filter. Two sources are considered to represent primary and a scattered radiations. Energy spectra taking into account the correlation between energy and diffusion angle have been used. Model parameters were tuned through a dose distribution iterative optimisation approach. The convergence condition rely on γ_{index} evaluation. The simulations were performed in two steps, phase space files were generated using `Geant4` toolkit, then energy deposit in water were computed using DPM code. Monte Carlo dose distributions of the model were compared to experimental data of two linac systems, an Elekta Synergy® with flattening filter and a Varian TrueBeam® with and without flattening filter. Good results were obtained in terms of γ_{index} 2%/2 mm criterion, dose difference and distance to agreement (DTA) analysis for field size range from 3×3 cm^2 to 30×30 cm^2.

1. Introduction

The great developments in computer technology during the last decades have made simulating a random process faster and more reliable. One of the most ingenious solutions implemented to model a system described by a stochastic behaviour is Monte Carlo technique [1]. This probabilistic approach is based on sampling pseudo-random sequences from a random number generator to simulate 'event by event' the described problem. The convergence of the calculated quantity and the corresponding statistical uncertainty is depending on the number of simulated events.

In radiation dosimetry, the use of Monte Carlo techniques has made possible the modelling of complex systems like linear accelerator or cyclotrons used to generate treatment beams. [2, 3]. Several measurable and non-measurable physical quantities could be estimated by simulation of particle transport. Moreover, correction factors of detectors used for beam calibration could be accurately calculated by Monte Carlo simulations which certainly contribute to improving absorbed dose measurements [4].

To make an efficient use of Monte Carlo methods for external radiation therapy for research or application purposes, a precise modelling of the beam source is mandatory [5, 6]. For accelerator

---

*Corresponding author

✉ zakaria.aboulbanine@gmail.com (Z. Aboulbanine)

ORCID(s): 0000-0002-5990-7999; 0000-0001-8633-2986

beams, the definition of the particle transverse distribution, the angular and the energy distributions is crucial to faithfully reproduce an experimental setup. The precision of the geometrical description of all components in a linear accelerator (linac) head or a cyclotron nozzle, impacts the accuracy of the calculated quantities of interest. Generally, such precise input requirements are not publicly available and are protected by manufacturers in case of commercial solutions, thus the development of alternatives making possible the simulation of radiation therapy beams is of great interest for the community.

The use of phase space files is one of the earliest optimisation options developed to efficiently simulate a radiation beam [3]. The principle consists in storing the main physical characteristics of particles passing across a scoring surface located usually at the linac exit window or upstream the secondary collimator. This technique leads to a considerable run time gain, for each new run the simulation starts from the phase space location downstream the previous simulated part. Primary particles are then loaded and sampled from the phase space file. Numerical approaches called Virtual Source Models, mainly developed for photon beams in Flattening Filter (FF) mode [7, 8, 9, 10, 11] or adapted to Free Flattening Filter (FFF) mode, have shown accurate results. The concept is based on representing the photon beam in the form of virtual sub-sources derived from measurements or phase space simulations [12, 13, 14, 15]. To improve computation performance, a virtual source model could be completed by a numerical collimator model [16, 17].

In this paper, we propose a 6 MV photon beam source model validated for both modes with FF and FFF. The source model derivation method is based only on measured dose distributions in water and do not require in-air dose measurements. The evaluation includes extensive simulations involving the model compared to experimental data of energy deposit in water. `Geant4` and DPM Monte Carlo codes were used for the validation process [18, 19]. Two linac configurations were investigated for a 6 MV nominal beam energy: Varian TrueBeam® for FF/FFF and Elekta Synergy® for FF mode.

2. Material and methods

2.1. Basic concept

In the present work, we aim to describe the methodology to build a simple and precise photon source model valid for 6 MV with and without Flattening filter. Two photon sources are considered, a primary source for Bremsstrahlung photons, and a secondary source for scattered radiations. Each of those two sub-sources is reconstructed from a photon fluence function and from correlated energy spectra. The fluence, the energy distributions and the corresponding parameters were identified to maximise γ_{index} evaluation for profiles and PDD curves at the central beam axis. The tuning was performed through a 2%/2 mm analysis for the large field 30×30 cm^2.

A reconstruction algorithm is used to determine the position, the direction and the energy of photons at a reference plane. The position will be sampled from a particle fluence distribution. The direction is defined in terms of a start point from which the radiation is emitted and its projection sampled from the fluence distribution at the reference plane fig. 1. Once the start and projection positions are determined the direction is directly calculated. The energy of a particle is randomly sampled from correlated energy distributions. A unique function has been used, one of its parameters is depending on the angular distribution. In order to simplify the model as much as possible while maintaining the highest achievable precision level, only five angular bins were considered.

2.2. Particle fluence model

As described in the previous subsection the proposed beam reconstruction approach requires the identification of the fluence distribution of particles at the source placement and its projection at
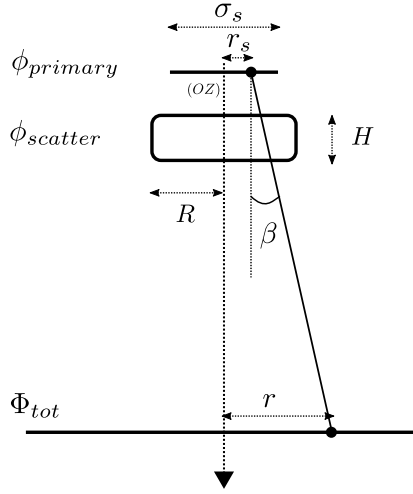
Figure 1: Geometric representation of the virtual sources used to reconstruct the photon beam. Photon direction is calculated in terms of the radial position r_s at the source and r the radial position at the reference reconstruction plane, β stands for the diffusion angle, σ_s is the size of the primary source, R and H are the dimensions of the scatter source.

a reference plane downstream. The source fluence ϕ_{source} eq. (1) and fig. 1 will be split into two components, a primary and scatter fluence :

$$\phi_{source} = \phi_{primary} + \phi_{scatter} \tag{1}$$

$\phi_{primary}$ is approximating the photon fluence at the base of the electron linac target. It will be described by a Gaussian distribution $\mathcal{G}(r_s|\mu_s, \sigma_s)$ eq. (2) centred around the central beam axis position μ_s in polar coordinate, with a standard deviation σ_s of 0.5 mm for Elekta Synergy® and 0.3 mm for Varian TrueBeam®. The parameter σ_s, commonly called spot size, is controlling penumbra effect [20].

$\phi_{scatter}$ is emulating the spatial distribution of photons scattered from different components in the linac head. In order to approximate the symmetry of the most contributing scatter sources, while keeping the simplicity of the model, a uniform cylindrical distribution was assumed. A radius $R = 10$ cm and a height $H = 21.7$ cm were considered as dimensions fig. 1. The optimisation of the scatter contribution enhances in particular the fluence variation around the field border and introduces an extra-focal aspect necessary to make the model more realistic.

$$\mathcal{G}(r_s|\mu_s, \sigma_s) = A_i \frac{1}{\sigma_s \sqrt{2\pi}} \exp\left[-\frac{1}{2}\left(\frac{r_s - \mu_s}{\sigma_s}\right)^2\right] \tag{2}$$

The radial distribution of primary and scattered photons at the reference reconstruction plane $\Phi_{tot,i}$ upstream the secondary collimator of the linac will be described as follows :

$$\Phi_{tot,i} = \Phi_{main,i} + \Phi_{c,i} \tag{3}$$

i stands for the beam mode FF or FFF.
$\Phi_{main,i}$ is the main fluence expression.
$\Phi_{c,i}$ is a correction function.
r is the radial position.

Table 1

Optimised parameters of Φ_{main} used to reconstruct the fluence eq. (4) at the reference plane.

p_j	$\Phi_{main,\text{FFF}}$	$\Phi_{main,\text{FF}}$
p_0	0.25	0.011
p_1 [mm]	4	1.85
p_2 [mm]	87	7
p_3	0.2	0.2

$$\Phi_{main,\text{FF}} = \frac{p_0}{2}\,\text{erf}\left(\frac{r-p_1}{p_2}\right) + p_3$$

$$\Phi_{main,\text{FFF}} = \frac{p_0}{2}\,\text{erfc}\left(\frac{r-p_1}{p_2}\right) + p_3 \tag{4}$$

$$\Phi_{c,\text{FF}} = r^3$$

$$\Phi_{c,\text{FFF}} = \mathcal{G}(r|\mu_r, \sigma_r)$$

$\Phi_{main,i}$ is given by the error function $\text{erf}(r)$ for FF mode and the complementary error function $\text{erfc}(r)$ for FFF mode eq. (4). This model have degrees of freedom to control the fluence variations in order to achieve a good match with the original beam particle fluence. For FF mode, the fluence is generally attenuated at the beam axis by the flattening filter component, this variation could be modelled by the $\text{erf}(r)$ shifted to the high fluence gradient position inside the beam, the width parameter is used to fit the attenuation effect. The fluence of FFF beams is characterised by a radial cone shape distribution [21, 22]. In order to reproduce this behaviour, a similar reasoning was adopted to model FFF fluence by shifted complementary error function $\text{erfc}(r)$.

p_0 parameter controls the amplitude of the error function. The second parameter p_1 shifts the function on the radial axis to fit the attenuation effect in case of FF beam or to fit as much as possible the cone beam shape for FFF beam. The parameter p_2 sets the width of the (complementary) error function. In this region the photon fluence increases slightly and gradually from the beam axis to the borders for flattened beams, the same effect could be seen in dose profile curves. p_3 with p_0 are used to adjust the difference between the maximal and minimal fluence values. The optimised parameters are given in table 1.

$\Phi_{c,i}$ is used to maximise the agreement of the reconstructed particle fluence with the real fluence of the accelerator based on the comparison of simulated and measured profiles at various depths, data of the large radiation field 30×30 cm^2 were used for this purpose. The radial position r of a sampled photon are multiplied by a scaling factor[1] depending on the reference plane position z along the beam axis. Since it is complicated to derive the correct distribution of the photon beam fluence for a direct comparison, measured and simulated dose distributions are evaluated instead.

The expression of the fluence correction function is depending on the photon beam mode. A third degree polynomial function has been used for the FF mode and a Gaussian distribution for the FFF mode. Those functions were chosen based on dose calculations involving only the first term $\Phi_{main,i}$. The shape of the correction function was then deduced from the deviations obtained through a comparison with reference profile data of the radiation field 30×30 cm^2. A tuning of the correction function parameters was done in order to maximise the agreement between simulated and measured dose in water.

---

[1]the scale factor is 0.25 for our case

Table 2

Contributions of the photon source fluence ϕ_{source} eq. (1) and the fluence at the reference reconstruction plane Φ_{tot} eqs. (3) and (4) for each linac or beam mode.

Fluence component	Beam mode		
	TrueBeam® FFF	FF	
		TrueBeam®	Elekta Synergy®
$\phi_{primary}$	80.0%	80.0%	75%
$\phi_{scatter}$	20.0%	20.0%	25%
Φ_{main}	99.9%	83%	80%
Φ_c	0.1%	17%	20%

The table 2 is summarising the probabilities considered for the photon source fluence ϕ_{source} eq. (1) and the reference plane photon fluence Φ_{tot} eq. (4) providing the best match between dose distributions of our model and measured data.

2.3. Correlated energy spectra

Total photon beam energy spectra were modelled in the literature using a log-normal [23, 24] or a modified log-normal function [25, 26]. It has also been demonstrated in previous studies that particle energy E is strongly dependent on the diffusion angle β [11, 27]. In this paper, to simplify as much as possible the model while taking into account this important aspect, energy distributions were considered as the product of two functions $P_1(E)$ and $P_{j,2}(E)$ correlated to the angular bin $\Delta\beta_j$ eq. (6).

The error function part $P_1(E)$ of the spectrum expression $P_j(E)$ eq. (5), is controlling the energy peak position and the weights of low energy range impacting much more buildup region for depth dose distributions. The exponential part $P_{j,2}(E)$ gives the possibility to tune the decay of the energy spectrum and optimise the penetration of the beam. This leads to maximising the agreement between MC energy deposit and experimental measurements beyond d_{max} the maximal dose depth.

$$P_j(E) = P_1(E) \times P_{2,j}(E) \tag{5}$$

$$P_1(E) = q_0 \left[1 + \mathrm{erf}\left(\frac{E - q_1}{q_2} \right) \right]$$
$$P_{2,j}(E) = \exp\left(-(E - q_1)q_{3,j} + q_4 \right) \tag{6}$$

The subscript j in eqs. (5) and (6) indicates the angular bin.
q_0 is an amplitude factor. q_1 and q_2 are respectively the shift and the width of the error function high gradient region, those parameters define the spectrum peak position fig. 2. q_3 and q_4 are used to adjust the decay rate of the exponential component eq. (6).

To take into account the correlation between energy and photon diffusion angle β, the range $[0, \beta_{max}]$ was discretized into non-linear angular bins, where β_{max} is the maximal diffusion angle. The number of bins and the corresponding width have been defined through an optimisation process fig. 3.

The invariant parameters of the energy spectra were identified through a trial and error process starting from initial parameters. The starting values are the result of fitting Monte Carlo energy spectra extracted from a 6 MV photon beam phase space of an Elekta Precise® linac available in the public International Atomic Energy Agency (IAEA) database [28]. A single energy spectrum is considered to find the best match between simulated and measured percent depth dose at central
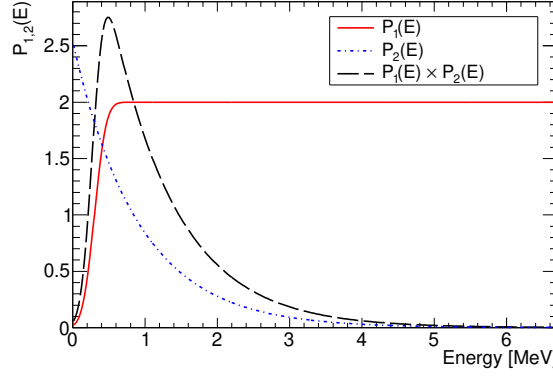
Figure 2: Decomposition of the energy spectrum function $P_j(E)$ used for the photon source model eqs. (5) and (6). The parameters for this demonstrative example are 1, 0.300, 0.180, 1.105 and 0.600 respectively for q_k, $k = \{0, 1, .., 4\}$.
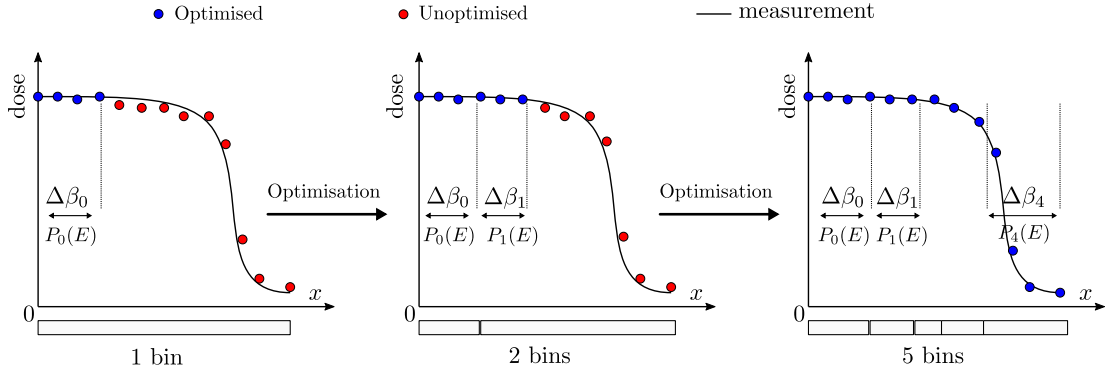
Figure 3: Dose distribution optimisation through iterative tuning of energy spectra parameter $q_{3,j}$ and the corresponding angular bin $\Delta\beta_j$. For each new iteration the angular bin number used in the simulations increases. The agreement between MC and measurements has been optimised within 2%/2 mm criterion with five angular bins for the large field size 30×30 cm^2.

beam axis. The optimisation process is summarised in the algorithms 1 and 2 in Appendix section. The convergence criterion is achieving 95% of points verifying $\gamma_{2\%/2\ mm} < 1$. The first part of the algorithm is optimising the parameters influencing more the buildup region $q_{\{0,1,2\}}$. The second part is tuning the rest of the parameters for the electronic equilibrium region.

A comparable procedure was used in order to obtain a good agreement between measured and simulated dose profiles at several depths: build-up, 10 cm and 20 cm. By considering the peak of the energy spectra located at $q_1 + q_2/2$, the distribution shift q_1 and q_4 as independent from the diffusion angle, we can optimise the simulated profile distributions by varying $q_{3,j}$. Five angular bins were considered to describe the correlation between the energy and the diffusion angle. The optimisation started by using only one spectrum, then the limit of the first angular bin are defined by the position from which $\gamma_{2\%/2\ mm}$ fails. For the second iteration, two angular bins are used and the same algorithm is then repeated till obtaining a $\gamma_{2\%/2\ mm}$ score at least equal to 95% fig. 3. The parameters obtained for the five energy spectra corresponding to the five angular bins are given in table 3.

Table 3
Optimised energy spectra parameters eqs. (5) and (6). TB and Syn in the table (c) refer respectively to Varian TrueBeam® and Elekta Synergy®

(a)

p_k	Beam Mode FFF	FF
q_0	0.02	0.02
q_1 [MeV]	0.55	0.58
q_2 [MeV]	0.1	0.18
$q_{3,j}$	table 3(b)	table 3(c)
q_4	0.6	0.6

(b)

	FFF	
$\Delta\beta_j$ [°]		$q_{3,j}$ [MeV^{-1}]
$\beta \leq 1.7°$		0.969
$]1.7, 3.1]°$		1.020
$]3.1, 8.0]°$		1.062
$]8.0, 9.3]°$		1.079
$\beta > 9.3°$		1.105

(c)

$\Delta\beta_j$ [°]	$q_{3,j}^{FF}$ [MeV^{-1}] TB	Syn
$\beta \leq 1.7°$	0.773	0.731
$]1.7, 3.1]°$	0.790	0.739
$]3.1, 5.6]°$	0.824	0.765
$]5.6, 8.4]°$	0.841	0.790
$\beta > 8.4°$	1.105	1.156

2.4. Beam reconstruction

The information of interest to be determined by the model will be the initial position, the direction and the energy of a generated photon fig. 4. The beam reconstruction method starts with sampling two points, a source point and and its projection on the reference reconstruction plane eqs. (1) and (3). The sampled positions are used to calculate the direction of the photon. The energy will be then randomly sampled from one of the five energy spectra correlated to the diffusion angle described in the previous subsection.
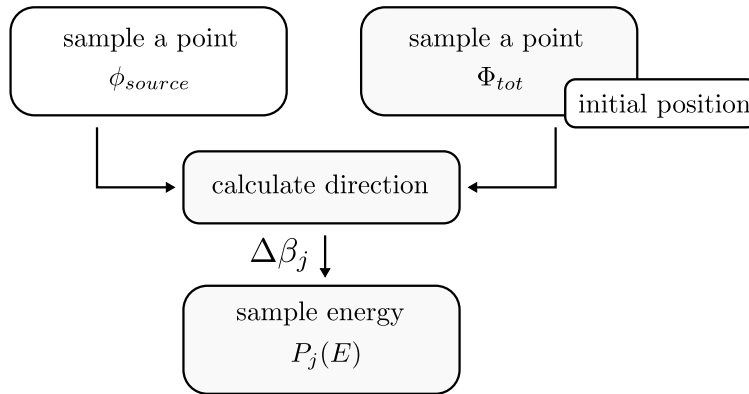
Figure 4: Photon source model reconstruction algorithm. The blocks in grey are showing the steps where output variables are calculated, position, direction and energy.

2.5. TrueBeam® data set

Commissioning data of the TrueBeam® system were retrieved from the Varian database[2] to validate the model for a large field size range. The measurements known as Representative Beam Data, were acquired using three linac units available at the same institution [29]. The data-set includes 6 MV dose distributions for FF and FFF photon beam modes. Profiles and percentage depth dose curves were measured using an IBA detector at a constant source-surface distance (SSD=100 cm). The ionisation chamber is a "CC13" with a sensitive volume of 0.13 cm^3 and inner radius of 0.305 cm.

2.6. Elekta Synergy® data set

Experimental dose measurements for the Elekta Synergy® 6 MV photon beam were performed at the radiotherapy department of Hassan II Oncology Centre in Oujda, Morocco. The linac delivers a

[2]https://www.myvarian.com

flattened 6 MV X-ray beam at a dose rate of 400 MU/min. A constant distance of 90 cm between the source and the water surface was considered. PDD and profile curves were measured using Semiflex 3D ionisation chamber type "PTW 31021" (PTW, Freiburg, Germany). It is a waterproof cylindrical chamber, with a nominal sensitive volume of 0.07 cm^3, an active length of 4.8 mm and a radius of 2.4 mm.

2.7. Monte Carlo simulations

The elaborated model is reconstructing the beam upstream the collimator. Two pairs of Tungsten jaws were used to set the radiation field size. The thickness of each jaw is 6.5 cm for TrueBeam® FFF and Elekta Synergy® FF, for TrueBeam® FF 6.2 cm has been used.

The validation computations were split into two phases. The first step is `Geant4` simulations [18] involving beam reconstruction using the source model, afterwards, particles are transported through the collimator geometry to generate a phase space downstream. For the second step, dose distributions in water were calculated using DPM code for a faster simulation [19].
A water phantom of $50 \times 50 \times 30$ cm^3 with a $2 \times 2 \times 2$ mm^3 dose resolution was used to score energy deposit. Four radiation field sizes were considered to cover the range from 3×3 cm^2 to 30×30 cm^2.

2.8. Accuracy evaluation

Dose calculated using the photon source model were compared to reference data of the Elekta Synergy® and Varian TrueBeam® by means of a global γ_{index} analysis [30], a relative dose difference for low dose gradient regions and distance to agreement in high dose gradient regions. For each radiation field the average $\langle \text{DTA} \rangle$ value and the relative error $\langle \Delta D \rangle$ were calculated eq. (7) over n points in this region. The corresponding minimum and maximum indicates the variation range of the quantity.

$$\langle \text{DTA} \rangle = \frac{1}{n} \sum_{i=0}^{n} \text{DTA}_i, \qquad \langle \Delta D \rangle = \frac{1}{n} \sum_{i=0}^{n} \Delta D_i \qquad (7)$$

The build-up of PDD and the penumbra of profile curves are qualified as high dose gradient locations and the places beyond d_{max} for PDD plots or data points inside the radiation field profile are considered as low dose gradient regions.

3. Results and discussion

The presented source model has been built based only on dose distribution measurements in water for 6 MV photon beams FF/FFF. The idea is a proof of concept showing the possibility to tune parameters describing photon fluence and energy distributions by an iterative dose distribution evaluation. The objective is to obtain those parameters for 6 MV nominal beam energy valid within the tolerance level 2%/2 mm. The reconstruction method gives in output the main photon characteristics : the initial position, the direction and the energy.

The final validation of the model was performed by calculating the γ_{index} distribution [30] for 3%/3 mm and 2%/2 mm criteria. Energy deposit statistical uncertainty of all Monte Carlo simulations reported in this paper is below 2% figs. 5 to 8. Results of γ_{index} evaluation are given in tables 4 and 5.

Elekta Synergy® percent depth dose 2%/2 mm analysis shows that at least 96% of data points are successfully passing the evaluation. This value was obtained for the small field 3×3 cm^2. For the same case, 3%/3 mm gives a probability of 99.3%. Simulated profile distributions are showing a high agreement with experimental data. More than 98% of profile points for all radiation fields have

Table 4
Percentage of dose distribution points successfully passing γ_{index} evaluation for Elekta Synergy® 6 MV FF photon beam.

| | | | field [cm^2] | | | |
			3×3 cm^2	10×10 cm^2	20×20 cm^2	30×30 cm^2
	d_{max}	2%/2 mm	100	100	100	100
		3%/3 mm	100	100	100	100
Profile	10 cm	2%/2 mm	100	100	100	100
		3%/3 mm	100	100	100	100
	20 cm	2%/2 mm	100	100	98.6	98.6
		3%/3 mm	100	100	100	100
Depth dose		2%/2 mm	96	98.7	98.7	98.7
		3%/3 mm	99.3	99.3	99.3	99.3

Table 5
Percentage of dose distribution points successfully passing γ_{index} evaluation for TrueBeam® 6 MV FF[FFF] photon beam.

| | | | field [cm^2] | | | |
			3×3 cm^2	10×10 cm^2	20×20 cm^2	30×30 cm^2
	d_{max}	2%/2 mm	100[100]	96[100]	100[99.3]	99.5[100]
		3%/3 mm	100[100]	100[100]	100[100]	100[100]
Profile	10 cm	2%/2 mm	100[100]	97.1[100]	100[100]	100[100]
		3%/3 mm	100[100]	100[100]	100[100]	100[100]
	20 cm	2%/2 mm	100[100]	99.1[100]	100[100]	97.5[97.4]
		3%/3 mm	100[100]	100[100]	100[100]	100[100]
Depth dose		2%/2 mm	99.3[99.3]	98.7[99.3]	98.7[99.3]	96.7[99.3]
		3%/3 mm	99.3[99.3]	99.3[99.3]	99.3[99.3]	98.7[99.3]

$\gamma_{2\%/2\ mm} < 1$ at all depths including d_{max} where the fluence and the corresponding energy spectra variations are critical.

The evaluation of Varian TrueBeam® FF/FFF is showing satisfactory results table 5. Percent depth dose curves at the central beam axis and profiles have a percentage of success at least equal to 96% for 2%/2 mm criterion.

The maximal DTA in average in the build-up region is less than 1.7 mm. Deeper locations beyond d_{max} has shown a maximal dose difference in average equal to 2.7% which is observed for the large radiation field of 30×30 cm^2. The mean DTA in penumbra regions and relative dose difference inside the radiation field were respectively less than 1.2 mm and 1% figs. 9 and 10.

The model presented in this work has been specifically designed to fit 6 MV photon beams for FF and FFF modes. The validation results has demonstrated the reliability and the efficiency of the source model tuning approach for a 6 MV nominal beam energy. It is also worth noting that the precision of the model is independent from most influencing parameters such as field size or calculation depth. In a future work further investigations will focus on the applicability of the presented source model for small field applications.

4. Conclusion

The methodology to establish a source model designed for 6 MV photon beams with and without flattening filter is presented. Two sources were considered, a focal source for primary photons and an extra-focal source for scattered photons. Analytical particle fluence functions and energy spectra correlated to the diffusion angle were used for the reconstruction of each beam component. Model parameters were tuned using energy deposit measurements in water for the radiation field 30×30 cm^2.

Extensive Monte Carlo simulations were carried out in order to validate the model for radiation fields from 3×3 cm^2 to 30×30 cm^2. The source model dose distributions were compared to experimental measurements in water for 6 MV photon beams of an Elekta Synergy® with flattening filter and a Varian TrueBeam® with and without flattening filter. Very good agreement has been obtained in terms of γ_{index} 2%/2 mm criterion for the simulated radiation fields. The $\gamma_{2\%/2\ mm}$ analysis has shown a probability of success greater or equal to 96 % for percent depth dose at the central beam axis and profiles at d_{max}, 10 cm and 20 cm depths. DTA analysis of high dose gradient locations were in average below 1.7 mm and 1.2 mm respectively for build-up and penumbra regions.

As a future perspective, the applicability and the efficiency of the model for small field Monte Carlo dosimetry could be studied.

5. Acknowledgements

A. Energy spectra optimisation algorithm

Algorithm 1: Optimisation of photon energy spectrum at the beam axis.

Result: Determine the parameters $p_{k=0,1..4}$ of eq. (5)
$i = 0$ // iteration index;
$N_i = 0$ // gamma index score vector;
$\Delta p_{k=0,1..4} = 0.2 \times p_{k=0,1..4}$ // optimisation step ;
convergence=false // convergence flag;
while *convergence==false* **do**
    phase_space=`Geant4_simulation`;
    dose_in_water=`DPM_simulation`(phase_space);
    // analyse percent depth dose at the beam axis (buildup);
    N_i =`gammaIndex`(dose_in_water, $z \leq z_{max}$);
    if $N_i < 95\%$ **then**
        `optimise`($p_{0,1,2}$, N_i);
    else
        // analyse percent depth dose at the beam axis (electronic equilibrium);
        N_i =`gammaIndex`(dose_in_water, $z > z_{max}$);
        if $N_i < 95\%$ **then**
            `optimise`($p_{4,5}$, N_i);
        else
            convergence = true;
        end
    end
end

**Algorithm 2:** `optimise`(p_k) function from algorithm 1.

function `optimise`(p_k, N_i);
if $N_i < N_{i-1}$ **then**
    $c = -1$;
    $\Delta p_k = \Delta p_{k,i-1} \times 0.8$;
else
    $c = 1$;
**end**
$p_k = p_k + c \times \Delta p_k$;
end function

References

[1] Alireza Haghighat. *Monte Carlo methods for particle transport*. Crc Press Boca Raton, FL, 2015.

[2] Barry L Werner, Faiz M Khan, and Firmin C Deibel. Model for calculating depth dose distributions for broad electron beams. *Medical physics*, 10(5):582–588, 1983.

[3] W Van der Zee and J Welleweerd. Calculating photon beam characteristics with monte carlo techniques. *Medical physics*, 26(9):1883–1892, 1999.

[4] Joao Seco and Frank Verhaegen. *Monte Carlo techniques in radiation therapy*. CRC press, 2013.

[5] X Allen Li, Lijun Ma, Shahid Naqvi, Rompin Shih, and Cedric Yu. Monte carlo dose verification for intensity-modulated arc therapy. *Physics in Medicine & Biology*, 46(9):2269, 2001.

[6] E Spezi, DG Lewis, and CW Smith. Monte carlo simulation and dosimetric verification of radiotherapy beam modifiers. *Physics in Medicine & Biology*, 46(11):3007, 2001.

[7] I Chetty, JJ DeMarco, and TD Solberg. A virtual source model for monte carlo modeling of arbitrary intensity distributions. *Medical physics*, 27(1):166–172, 2000.

[8] Michael K Fix, Paul J Keall, Kathryn Dawson, and Jeffrey V Siebers. Monte carlo source model for photon beam radiotherapy: photon source characteristics: Monte carlo source model. *Medical physics*, 31(11):3106–3121, 2004.

[9] W González, IB García-Ferreira, M Anguiano, and AM Lallena. A general photon source model for clinical linac heads in photon mode. *Radiation Physics and Chemistry*, 117:140–152, 2015.

[10] Jason Cashmore, Sergey Golubev, Jose Luis Dumont, Marcin Sikora, Markus Alber, and Mark Ramtohul. Validation of a virtual source model for monte carlo dose calculations of a flattening filter free linac. *Medical physics*, 39(6Part1):3262–3269, 2012.

[11] L Grevillot, T Frisson, D Maneval, N Zahra, JN Badel, and D Sarrut. Simulation of a 6 mv elekta precise linac photon beam using gate/geant4. *Physics in Medicine & Biology*, 56(4):903, 2011.

[12] Zhen Tian, Yongbao Li, Michael Folkerts, Feng Shi, Steve B Jiang, and Xun Jia. An analytic linear accelerator source model for gpu-based monte carlo dose calculations. *Physics in Medicine & Biology*, 60(20):7941, 2015.

[13] Obioma Nwankwo, Gerhard Glatting, Frederik Wenz, and Jens Fleckenstein. A single-source photon source model of a linear accelerator for monte carlo dose calculation. *PloS one*, 12(9):e0183486, 2017.

[14] Deae-eddine Krim, Abdeslem Rrhioua, Mustapha Zerfaoui, and Dikra Bakari. Development of a new hybrid virtual source model to simulate elekta synergy mlci2 linac. *Radiation Measurements*, page 106780, 2022.

[15] James R Castle, Jingwei Duan, Xue Feng, and Quan Chen. Development of a virtual source model for monte carlo-based independent dose calculation for varian linac. *Journal of Applied Clinical Medical Physics*, page e13556, 2022.

[16] Jiankui Yuan, Yi Rong, and Quan Chen. A virtual source model for monte carlo simulation of helical tomotherapy. *Journal of applied clinical medical physics*, 16(1):69–85, 2015.

[17] Zakaria Aboulbanine and N El Khayati. A theoretical multileaf collimator model for fast monte carlo dose calculation of linac 6/10 mv photon beams. *Biomedical Physics & Engineering Express*, 5(5):055004, 2019.

[18] Sea Agostinelli, John Allison, K al Amako, John Apostolakis, H Araujo, P Arce, M Asai, D Axen, S Banerjee, G 2 Barrand, et al. Geant4âĂŤa simulation toolkit. *Nuclear instruments and methods in physics research section A: Accelerators, Spectrometers, Detectors and Associated Equipment*, 506(3):250–303, 2003.

[19] Josep Sempau, Scott J Wilderman, and Alex F Bielajew. Dpm, a fast, accurate monte carlo code optimized for photon and electron radiotherapy treatment planning dose calculations. *Physics in Medicine & Biology*, 45(8):2263, 2000.

[20] A Toutaoui, N Khelassi-Toutaoui, B Hattali, et al. Monte carlo photon beam modeling and commissioning for radiotherapy dose calculation algorithm. *Physica Medica*, 30(7):833–837, 2014.

[21] Mårten Dalaryd, Gabriele Kragl, Crister Ceberg, Dietmar Georg, Brendan McClean, Sacha af Wetterstedt, Elinore Wieslander, and Tommy Knöös. A monte carlo study of a flattening filter-free linear accelerator verified with measurements. *Physics in Medicine & Biology*, 55(23):7333, 2010.

[22] S Valdenaire, H Mailleux, and P Fau. Modeling of flattening filter free photon beams with analytical and monte carlo tps. *Biomedical Physics & Engineering Express*, 2(3):035010, 2016.

[23] Peter Bloch and James McDonough. Extraction of the photon spectra from measured beam parameters. *Medical physics*, 25(5):752–757, 1998.

[24] J Yang, JS Li, L Qin, W Xiong, and CM Ma. Modelling of electron contamination in clinical photon beams for monte carlo dose calculation. *Physics in Medicine & Biology*, 49(12):2657, 2004.

[25] W Ulmer, J Pyyry, and W Kaissl. A 3d photon superposition/convolution algorithm and its foundation on results of monte carlo calculations. *Physics in Medicine & Biology*, 50(8):1767, 2005.

[26] M Sikora, O Dohm, and M Alber. A virtual photon source model of an elekta linear accelerator with integrated mini mlc for monte carlo based imrt dose calculation. *Physics in Medicine & Biology*, 52(15):4449, 2007.

[27] Zakaria Aboulbanine and Naïma El Khayati. Validation of a virtual source model of medical linac for monte carlo dose calculation using multi-threaded geant4. *Physics in Medicine & Biology*, 63(8):085008, 2018.

[28] R Capote, R Jeraj, CM Ma, D WO Rogers, F Sánchez-Doblado, J Sempau, J Seuntjens, and JV Siebers. Phase-space database for external beam radiotherapy. summary report of a consultants' meeting. 2006.

[29] Zheng Chang, Qiuwen Wu, Justus Adamson, Lei Ren, James Bowsher, Hui Yan, Andrew Thomas, and Fang-Fang Yin. Commissioning and dosimetric characteristics of truebeam system: composite data of three truebeam machines. *Medical physics*, 39(11):6981–7018, 2012.

[30] Daniel A Low, William B Harms, Sasa Mutic, and James A Purdy. A technique for the quantitative evaluation of dose distributions. *Medical physics*, 25(5):656–661, 1998.
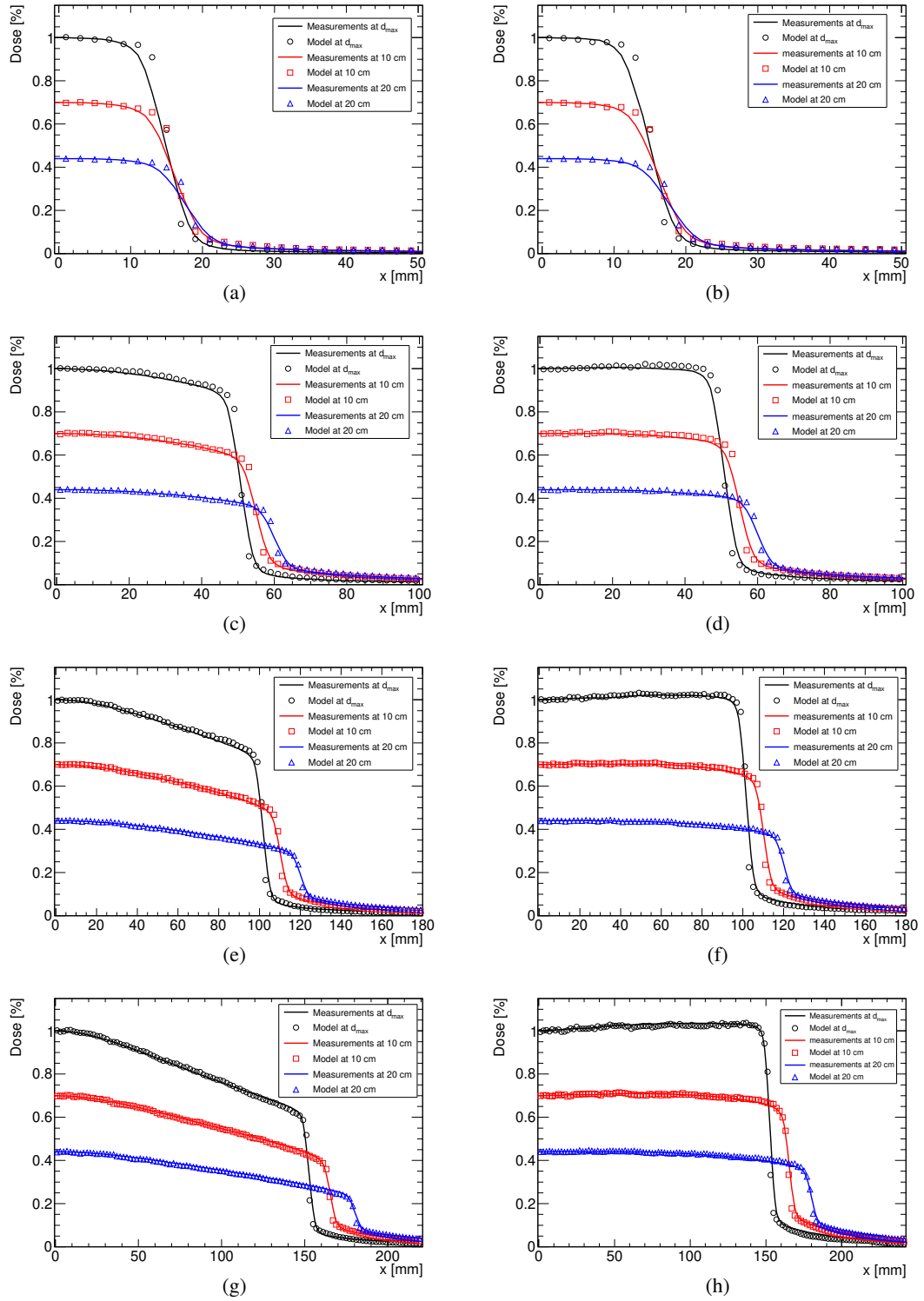
Figure 5: Dose profile distributions for Varian TrueBeam® 6 MV FF (right) and FFF (left) photon beam at three depths : d_{max}, 10 cm and 20 cm. Solid lines refer to experimental measurements and markers correspond to MC simulations. (a, b) : 3×3 cm²; (c, d) : 10×10 cm²; (e, f) : 20×20 cm²; (g, h) : 30×30 cm².
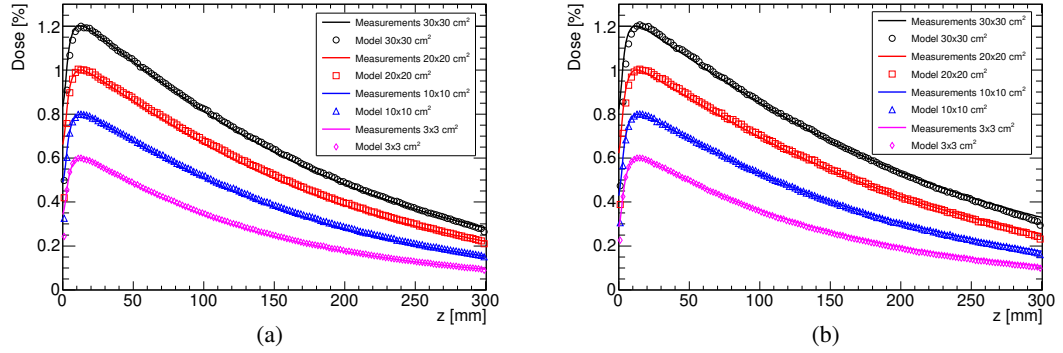
Figure 6: Percent depth distributions for Varian TrueBeam® 6 MV FFF (a) and Varian TrueBeam® FF (b). Solid lines refer to experimental measurements and markers correspond to MC simulations for various field sizes.
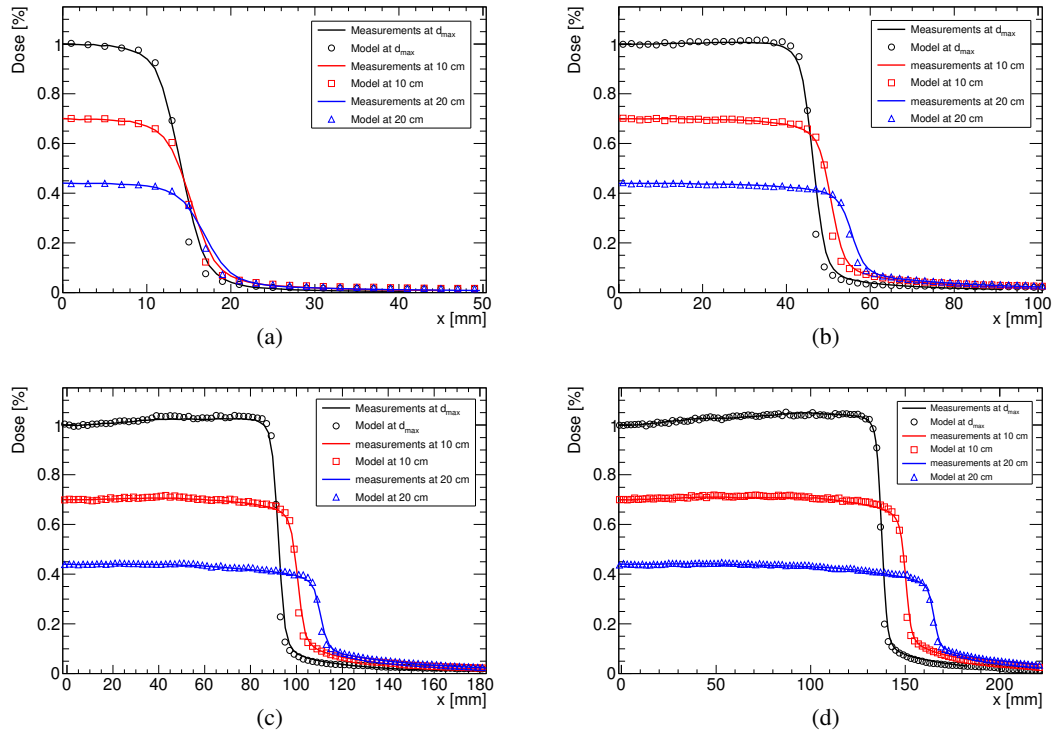

Figure 7: Dose profile distributions for Elekta Synergy® 6 MV FF photon beam at three depths : d_{max}, 10 cm and 20 cm. Solid lines refer to experimental measurements and markers correspond to MC simulations. (a) : 3×3 cm^2; (b) : 10×10 cm^2; (c) : 20×20 cm^2; (d) : 30×30 cm^2.
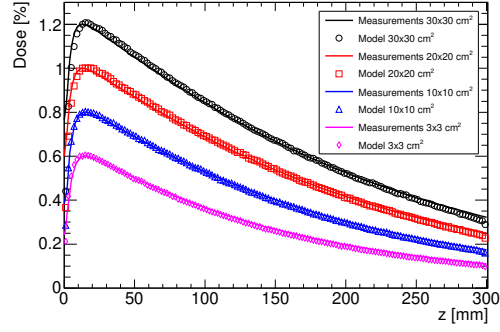
Figure 8: Percent depth distributions for Elekta Synergy® 6 MV FF. Solid lines refer to experimental measurements and markers correspond to MC simulations for various field sizes.
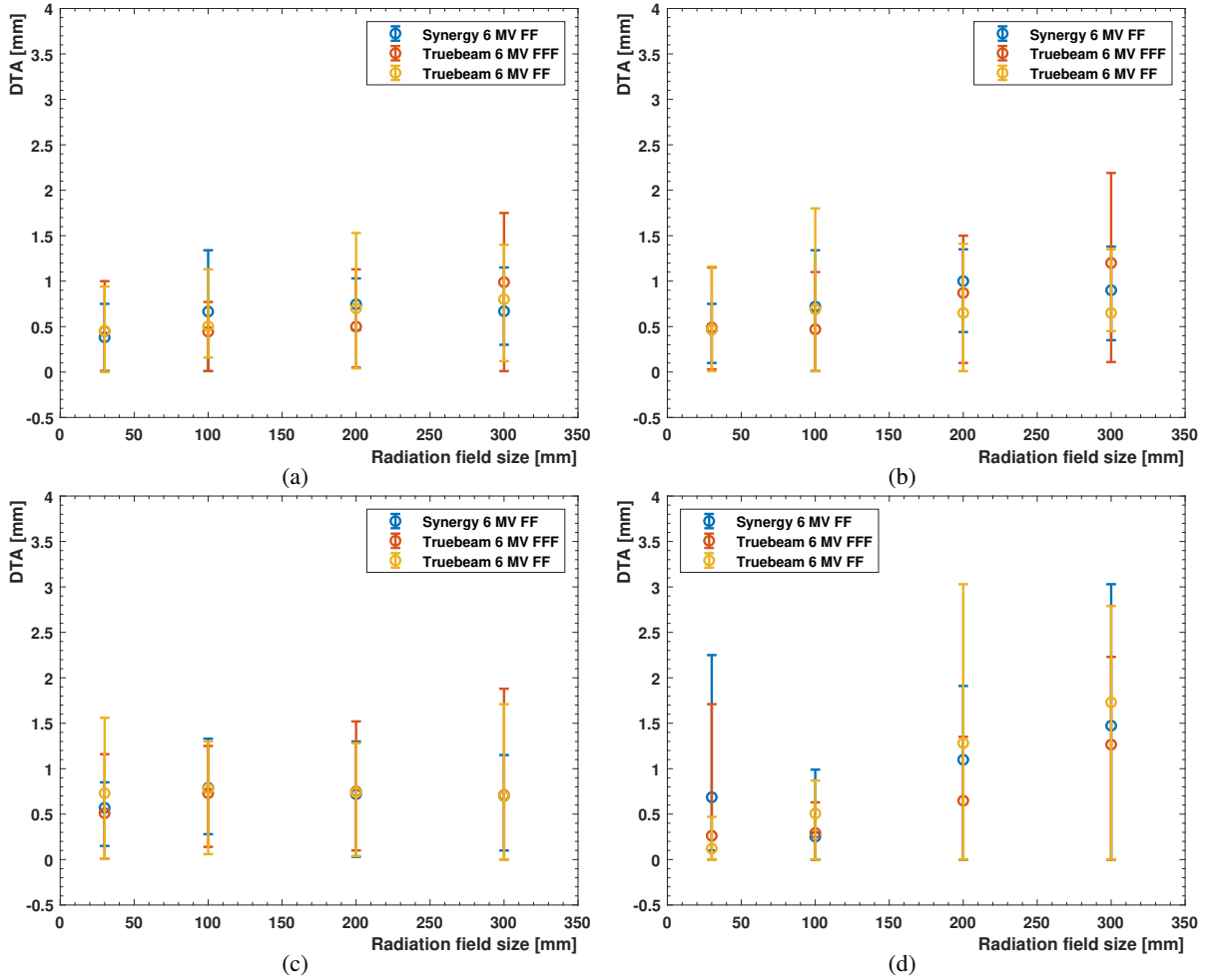
Figure 9: Distance To Agreement (DTA) analysis in high dose gradient regions versus the radiation field size, points correspond to the average value and error bars to maximal and minimal values. (a,b,c) analysis for penumbra profiles at d_{max}, 10 cm and 20 cm depth; (d) : analysis of the PDD in the buildup region.
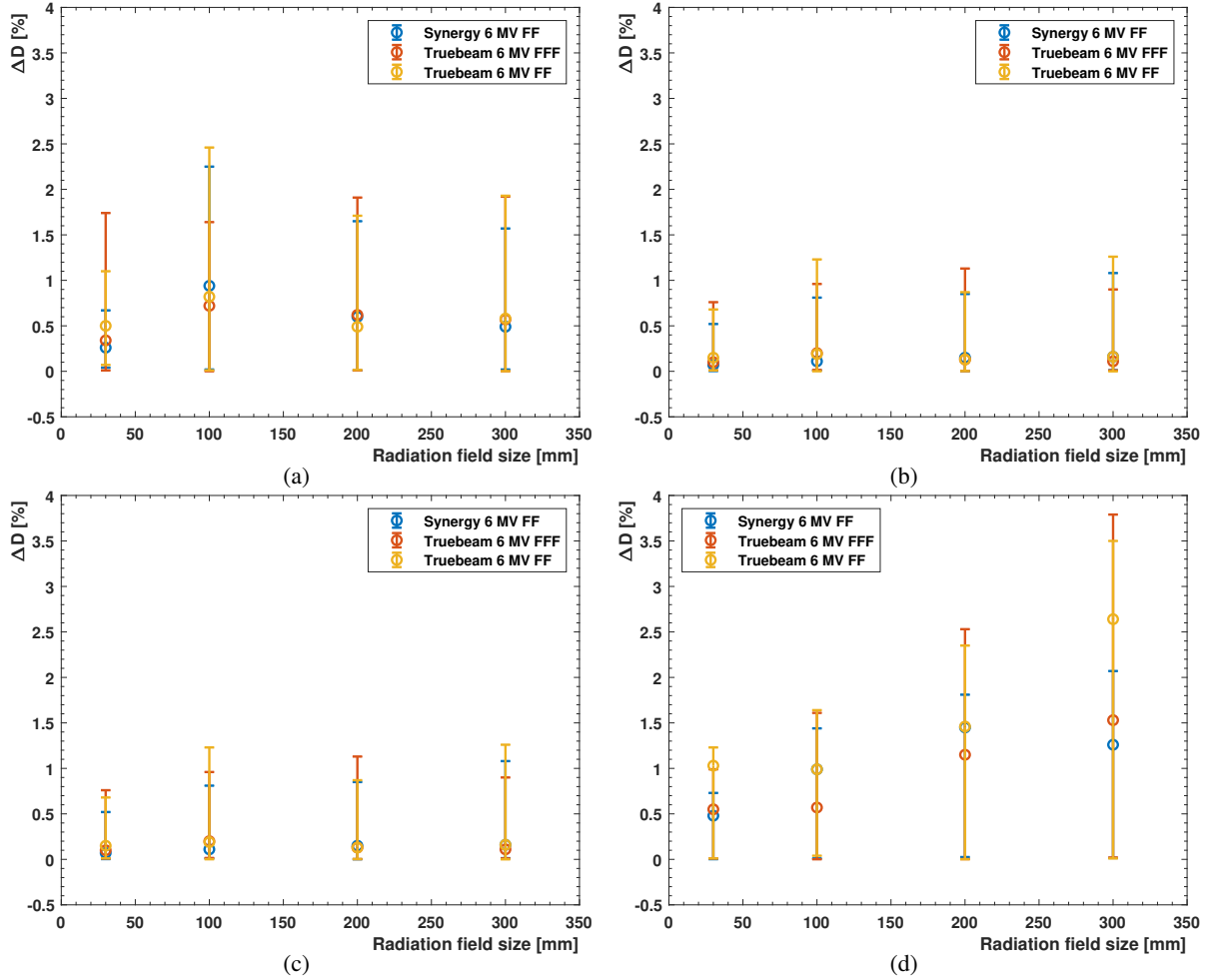
Figure 10: Relative dose difference analysis in low dose gradient regions versus the radiation field size, points correspond to the average value and error bars to maximal and minimal values. (a,b,c) analysis for profiles at d_{max}, 10 cm and 20 cm depth; (d) : analysis of the PDD beyond d_{max} depth.